Nuclear dependence coefficient $\alpha(A,q_T)$ for Drell-Yan and J/ψ production

Xiaofeng Guo
Department of Physics and Astronomy, University of Kentucky, Lexington, Kentucky 40506

Jianwei Qiu and Xiaofei Zhang
Department of Physics and Astronomy, Iowa State University, Ames, Iowa 50011

(Received 15 December 1999; published 26 July 2000)

Define the nuclear dependence coefficient $\alpha(A,q_T)$ in terms of the ratio of the transverse momentum spectrum in hadron-nucleus and in hadron-nucleon collisions $d\sigma^{hA}/dq_T^2/d\sigma^{hN}/dq_T^2 \equiv A^{\alpha(A,q_T)}$. We argue that, in the small q_T region, the $\alpha(A,q_T)$ for the Drell-Yan and J/ψ production is given by a universal function $a+bq_T^2$, where the parameters a and b are completely determined by either calculable quantities or independently measurable physical observables. We demonstrate that this universal function $\alpha(A,q_T)$ is insensitive to A for normal nuclear targets. For a color deconfined nuclear medium, $\alpha(A,q_T)$ becomes strongly dependent on A. We also show that our $\alpha(A,q_T)$ for the Drell-Yan process is naturally linked to the perturbatively calculated $\alpha(A,q_T)$ at large q_T without any free parameters, and $\alpha(A,q_T)$ is consistent with E772 data for all q_T.

PACS number(s): 12.38.−t, 11.80.La, 13.85.Qk, 24.85.+p

I. INTRODUCTION

It has long been observed that in high-energy hadron-nucleus collisions the transverse momentum spectra of produced particles differ significantly from those in hadron-nucleon collisions [1,2]. This anomalous nuclear dependence is known as the Cronin effect. In recent years, much data on such nuclear dependence for the Drell-Yan [3–5] and J/ψ production [6–8] became available, and these new data have renewed our interest to understand the observed novel effect [9]. Although it is believed that the Cronin effect is a result of parton multiple scattering inside a nuclear medium, systematic calculations in QCD for such anomalous nuclear dependence only exist for the large transverse momentum (q_T) region [10–12], but not for the small q_T region due to technical difficulties in handling multiscale calculations in QCD perturbation theory. In this paper, we derive the nuclear dependence in transverse momentum distributions for the Drell-Yan and J/ψ production in the small q_T region by combining constraints from perturbatively calculable quantities in the large q_T region and the available information from independently measured physical observables [13].

In high-energy nuclear collisions, in addition to short-distance single scattering, parton multiple scattering becomes very important. According to QCD factorization theorem [14], physical observables due to single hard scattering in hadronic collisions depend on the parton distributions. In terms of generalized QCD factorization theorem [15], contributions to physical observables from parton multiple scattering are directly proportional to multiparton correlation functions. These correlation functions are as fundamental as the parton distributions, and they provide complementary information on nonperturbative QCD dynamics [16]. Since single hard scattering is localized in position space, it is the multiple scattering that is sensitive to the size of nuclear medium, and is therefore responsible for the anomalous nuclear dependence. Measurements of such anomalous nuclear dependence provide a window of opportunities to explore the dynamics of parton correlations, which have important implications for the physics in relativistic heavy ion collisions.

The nuclear dependence of the transverse momentum spectrum is often presented in terms of the ratio of cross sections R or the nuclear dependence coefficient α. For example, for the Drell-Yan pair production, R and α are defined by

$$R(A,q_T) \equiv \frac{1}{A}\frac{d\sigma^{hA}}{dQ^2\,dq_T^2}\Big/\frac{d\sigma^{hN}}{dQ^2\,dq_T^2} \equiv A^{\alpha(A,q_T)-1}, \quad (1)$$

where Q and q_T are the Drell-Yan pair's total invariant mass and transverse momentum, respectively, and A is the atomic weight of the nuclear target. In Eq. (1), $d\sigma^{hA}/dQ^2\,dq_T^2$ and $d\sigma^{hN}/dQ^2\,dq_T^2$ are the transverse momentum spectrum in hadron-nucleus and hadron-nucleon collisions, respectively. Since single hard scattering is localized in space, both $R(A,q_T)$ and $\alpha(A,q_T)$ should be very close to 1 if there is no multiple scattering. However, data on the ratio of the Drell-Yan transverse momentum spectrum show that $R(A,q_T)$ very much differs from one [or $\alpha(A,q_T)$ is significant away from 1] [4]. In Ref. [4], data on $R(A,q_T)$ shows a nontrivial dependence on both A and q_T for different nuclear targets (including C, Ca, Fe, and W). In terms of $\alpha(A,q_T)$, the Drell-Yan data has the following general features: $\alpha(A,q_T=0)$ is less than 1, it increases as q_T increases, and it can be as large as 1.07 [3–5].

When q_T is large ($\sim Q$), the q_T dependence of $\alpha(A,q_T)$ can be calculated within QCD perturbation theory, and a significant nuclear enhancement in $\alpha(A,q_T)$ was predicted [11]. Although it was argued in Ref. [11] that in the small q_T region, the $\alpha(A,q_T)$ or the transverse momentum spectrum should show nuclear suppression, no quantitative analysis or prediction was given for the suppression. Since almost all existing data on the nuclear dependence of the Drell-Yan production are in the small q_T region [3–5], it is very important to derive a quantitative description of the nuclear dependence coefficient $\alpha(A,q_T)$ or the ratio $R(A,q_T)$ for the small q_T region.

Furthermore, J/ψ data in hadron-nucleus collisions show that the $\alpha(A,q_T)$ [or $R(A,q_T)$] for J/ψ production as a function of q_T has similar features as that of the $\alpha(A,q_T)$ [or $R(A,q_T)$] for the Drell-Yan production [7,8]. Recent data from Fermilab experiment E866 show that $\alpha(A,q_T)$ for J/ψ production has a universal shape, but its magnitude depends on the range of x_F [6]. J/ψ suppression in relativistic heavy ion collisions was predicted to signal the color deconfinement [17]. Recently, significant J/ψ suppression has been observed in existing fixed target experiments [18,19]. The data have generated a lot of theoretical discussions in searching for the mechanism of the observed J/ψ suppression. Understanding the features in $\alpha(A,q_T)_{J/\psi}$ is very valuable for such investigations.

In this paper, we argue that in the small q_T region, $\alpha(A,q_T)$ for the Drell-Yan production is given by an universal function $a_1+b_1\ q_T^2$, where a_1 and b_1 are completely determined by the measured ratio of total cross sections $d\sigma^{hA}/dQ^2/d\sigma^{hN}/dQ^2$, and the averaged transverse momentum square $\langle q_T^2\rangle_{\rm DY}^{hN}$ in hadron-nucleon collisions, plus perturbatively calculable quantities, such as the transverse momentum broadening $\Delta\langle q_T^2\rangle_{\rm DY}$ in hadron-nucleus collisions. The $\langle q_T^2\rangle_{\rm DY}^{hN}$ and $\Delta\langle q_T^2\rangle_{\rm DY}$ will be defined in Eqs. (7) and (12).

According to the generalized QCD factorization theorem [15], as with all perturbatively calculable hadronic quantities, the transverse momentum broadening for the Drell-Yan production $\Delta\langle q_T^2\rangle_{\rm DY}$ can be factorized into a convolution of an infrared safe hard part and corresponding universal quark-gluon correlation functions. The infrared safe hard part is calculable in QCD perturbation theory and was derived in Ref. [20]. Although the quark-gluon correlation functions are nonperturbative in nature and unknown, just like the well-known parton distributions, these functions are universal and they appear in the factorized expressions of other physical observables. For example, the same quark-gluon correlation functions in the expression for $\Delta\langle q_T^2\rangle_{\rm DY}$ appear in the factorized formulas for the $\alpha(A,q_T)$ in the large q_T region [11]. Because of the universality of these quark-gluon correlation functions, the data on $\Delta\langle q_T^2\rangle_{\rm DY}$ can be used to extract the quark-gluon correlation functions, which can then be used to predict $\alpha(A,q_T)$ in the large q_T region. In this paper, we show that the Fermilab E772 data on $\Delta\langle q_T^2\rangle_{\rm DY}$ can be used to extract the size of the quark-gluon correlation functions, which can then be used to predict the $\alpha(A,q_T)$ in the small q_T region.

We further demonstrate that our $\alpha(A,q_T)$ for the Drell-Yan production in small q_T region is naturally connected to the perturbatively calculated $\alpha(A,q_T)$ in the large q_T region, and we also show that the predicted $\alpha(A,q_T)$ is consistent with the E772 data in both the small and large q_T regions. Furthermore, we show that although the ratio of the transverse momentum spectrum $R(A,q_T)$ can have a nontrivial dependence on the atomic weight A, the nuclear dependence coefficient $\alpha(A,q_T)$ is *insensitive* to the atomic weight A for normal nuclear targets. On the other hand, we argue that in a color deconfined nuclear medium, the $\alpha(A,q_T)$ becomes very sensitive to the A due to a long range color correlation.

In addition, we show that $\alpha(A,q_T)$ for J/ψ production in small q_T region is given by the same functional form: $a_2+b_2\ q_T^2$, and the new parameters a_2 and b_2 are also completely determined by the ratio of total cross sections $\sigma_{J/\psi}^{hA}/\sigma_{J/\psi}^{hN}$ and the averaged transverse momentum square $\langle q_T^2\rangle_{J/\psi}^{hN}$ in hadron-nucleon collisions, plus perturbatively calculable quantities, such as the transverse momentum broadening $\Delta\langle q_T^2\rangle_{J/\psi}$ in hadron-nucleus collisions. Our predictions for $\alpha_{J/\psi}(A,q_T)$ are consistent with recent data from Fermilab E866.

The predicting power of our nuclear dependence coefficient function $\alpha(A,q_T)$ for the Drell-Yan and J/ψ production is its universal quadratic dependence on q_T, and the fact that all parameters are completely fixed by either calculable or independently measurable quantities. In addition, we predict that the $\alpha(A,q_T)$ is extremely insensitive to the atomic number A for normal nuclear targets while it can be very sensitive to A (or the medium size) for a color deconfined medium.

The rest of this paper is organized as follows. In the next section, we argue that the Drell-Yan transverse momentum spectrum in hadron-nucleon and hadron-nucleus collisions should be well represented by a Gaussian-like distribution in the small q_T region at fixed target energies. From such a transverse momentum spectrum, we derive a universal expression of $\alpha(A,q_T)$ for the Drell-Yan production in the small q_T region in Sec. III. We explicitly demonstrate that the $\alpha(A,q_T)$ is insensitive to the atomic weight A, and the $\alpha(A,q_T)$ in the small q_T region is naturally connected to the perturbatively calculated $\alpha(A,q_T)$ in the large q_T region. We then compare our universal function $\alpha(A,q_T)$ with E772 data at all q_T. In Sec. IV, we provide $\alpha(A,q_T)$ for J/ψ production, and discuss the similarity and difference between the $\alpha(A,q_T)$ for the Drell-Yan and J/ψ production. We show that in a color deconfined nuclear medium, the $\alpha(A,q_T)$ for J/ψ production becomes very sensitive to the atomic number A (or the medium size), while it is extremely insensitive to the A for normal color confined nuclear targets. Finally, in Sec. V, we summarize our main conclusions, and discuss the predicting power of our nuclear dependence coefficient $\alpha(A,q_T)$.

II. THE DRELL-YAN TRANSVERSE MOMENTUM SPECTRUM

Depending on physics origins, the Drell-Yan transverse momentum spectrum can be divided into three regions, as shown in Fig. 1. The small q_T region corresponds to the region where $q_T<q_T^S\sim 1$ GeV. The spectrum in this region, labeled by I in Fig. 1, is dominated by the intrinsic transverse momenta of colliding partons. At leading order in perturbation theory, the Drell-Yan transverse momentum distribution is given by

$$\frac{d\sigma^{hN}}{dQ^2\,d^2q_T}=\frac{d\sigma_{hN}}{dQ^2}\,\delta^2(\vec{q}_T). \tag{2}$$

The effect of the parton intrinsic transverse momentum can

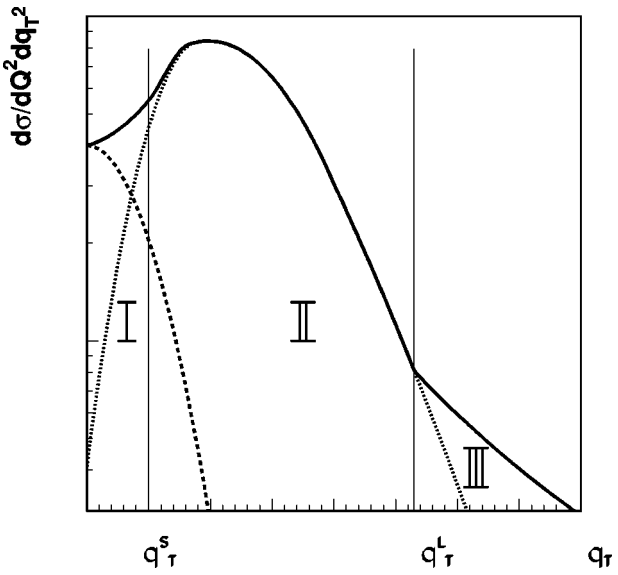

FIG. 1. Typical Drell-Yan transverse momentum spectrum as a function of q_T in three regions.

be included by replacing the δ function in Eq. (2) by its Gaussian-representation, $\delta(q_x)=\lim_{\tau\to 0}(1/\sqrt{2\pi}\tau)\exp[-q_x^2/2\tau^2]$ [21], and we obtain

$$\frac{d\sigma^{(I)}}{dQ^2\,dq_T^2}=N_{\rm DY}\frac{1}{2\tau^2}e^{-q_T^2/2\tau^2}, \tag{3}$$

where the superscript (I) indicates region I, $N_{\rm DY}$ is a dimensional normalization, and τ is the width of the Gaussian-like distribution. The physical meaning of the $N_{\rm DY}$ and τ will be determined later. In principle, $N_{\rm DY}$ and τ are nonperturbative quantities.

The intermediate q_T region, labeled by II in Fig. 1, corresponds to the region where $q_T^S \leqslant q_T \leqslant q_T^L$ with $q_T^L \equiv \kappa Q$ and $\kappa \sim 1/3-1/2$. In this region, the physically observed scales: Q and q_T are both large enough, and in principle, QCD perturbation theory can be used to calculate the short-distance partonic scattering and the Drell-Yan cross section can be factorized into the following form [14]:

$$\frac{d\sigma^{hN}}{dQ^2\,dq_T^2}=\sum_{a,b}\ \phi_{a/h}(x',\mu^2)\otimes\phi_{b/N}(x,\mu^2) \otimes\frac{d\hat{\sigma}^{ab}}{dQ^2\,dq_T^2}\left(x',x,\alpha_s(\mu^2),\frac{Q^2}{\mu^2},\frac{q_T^2}{\mu^2}\right), \tag{4}$$

where $\Sigma_{a,b}$ sum over all parton flavors a and b, the μ represents both the renormalization and factorization scales, the ϕ's and $\otimes$'s represent the parton distributions and the convolution over incoming partons' momentum fractions, respectively. In Eq. (4), the $d\hat{\sigma}^{ab}/dQ^2\,dq_T^2$ is a short-distance contribution for partons a and b to produce a Drell-Yan lepton pair, and it can be calculated perturbatively in terms of a power series of the strong coupling constant $\alpha_s(\mu^2)$ with the coefficients that depend logarithmically on the ratio of scales Q^2/μ^2 and q_T^2/μ^2. The scale μ can be chosen to be equal to Q or q_T, or somewhere between, and the factorized Drell-Yan cross section in Eq. (4) should not be sensitive to a specific choice of the scale if the factorized expression is reliable.

If the Q is much larger than the q_T, the perturbatively calculated $d\hat{\sigma}^{ab}/dQ^2\,dq_T^2$ will have large logarithms, such as $\ln(Q^2/q_T^2)$, for any choice of the scale μ. These large logarithms are due to the gluon radiation off the incoming partons before the hard collision takes place to produce a Drell-Yan lepton pair [22,23]. Because of the infrared and collinear singularities associated with the massless gluons, we can have two powers of the large logarithms for every power of the strong coupling constant α_s in the perturbatively calculated $d\hat{\sigma}^{ab}/dQ^2\,dq_T^2$. Clearly, the logarithms $[\alpha_s\ln^2(Q^2/q_T^2)]^n$, can be larger than the unity if the Q is much larger than the q_T. For example, for Z^0 production at the Fermilab Tevatron energies, the ratio Q^2/q_T^2 can be as large as 8×10^3 for $q_T\sim 1$ GeV and $Q\sim 91$ GeV. Consequently, the high order corrections in α_s can be as important as the lower order terms, and therefore, the perturbatively calculated $d\hat{\sigma}^{ab}/dQ^2\,dq_T^2$ at a fixed order of α_s^n are no longer reliable.

Using the renormalization group method, the large logarithms $[\alpha_s\ln^2(Q^2/q_T^2)]^n$ in the perturbatively calculated $d\hat{\sigma}^{ab}/dQ^2\,dq_T^2$ can be resummed to all orders in α_s [22,23]. As pointed out in Ref. [23], the resummation of the large logarithms can be systematically carried out by solving a corresponding renormalization group equation in b space, which is the Fourier transform of the transverse momentum q_T space. The kernel of the renormalization group equation can be calculated order by order in α_s in QCD perturbation theory. In order to obtain the Drell-Yan transverse momentum distribution, one has to perform the Fourier transform of the b-space solution of the renormalization group equation back to the q_T space; and it is necessary to have the b-space solution for all values of b. However, since the kernel was calculated in perturbative QCD, the b-space solution is only reliable for small values of b (i.e., $b\ll 1/\Lambda_{\rm QCD}$). Therefore, a nonperturbative function $F^{\rm NP}(b)$ had to be introduced to cover the large b region [23]. The parameters in the $F^{\rm NP}(b)$ were determined by fitting experimental data on the Drell-Yan q_T spectrum [24,25]. The role of this nonperturbative function $F^{\rm NP}(b)$ is similar to that of the input parton distributions $\phi(x,Q_0^2)$ when we solve the renormalization group equations [or the Dokshitzer-Gribov-Lipatov-Altarelli-Parisi (DGLAP) equations] for the parton distributions' Q^2 dependence.

As argued in Ref. [23], the nonperturbative $F^{\rm NP}(b)$ should have a Gaussian form in b space. Since large b values correspond to a small q_T region after the Fourier transform, the Gaussian form of $F^{\rm NP}(b)$ is consistent with our q_T spectrum in region (I). Furthermore, the Drell-Yan q_T spectrum in region (II) at fixed target energies is mainly determined by the resummed b-space distribution in large b region, which is completely dominated by the shape of $F^{\rm NP}(b)$. Consequently, the resummation performed in the small b region

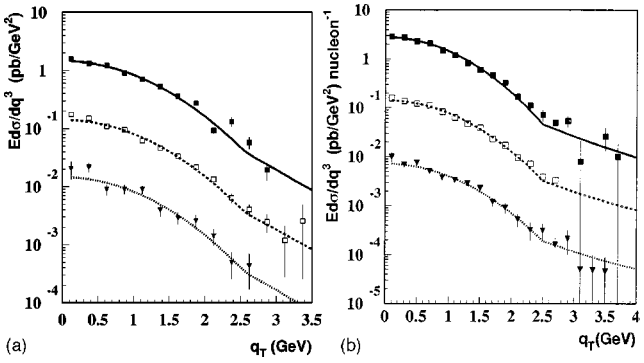

FIG. 2. Data on the Drell-Yan transverse momentum spectrum: (a) E772 [26] and (b) CFS [27], in comparison with a Gaussian-like fit in the small q_T region plus a calculated perturbative tail in the large q_T region.

does not have any noticeable effect on the low q_T spectrum at fixed target energies. Experimentally, all existing data for the Drell-Yan continuum between J/ψ and Υ peak at fixed target energies [3,4] can be well represented by the Gaussian-like q_T distribution for $q_T < q_T^L$. In Fig. 2, we show that the Drell-Yan data at both 800 [26] and 400 GeV [27] can be well represented by a Gaussian-like fit for q_T up to 2.5 GeV, and $Q=5.5$, 8.5, and 11.5 GeV, respectively. The widths of the Gaussian-like fits in Fig. 2 are consistent with the parameters in the $F^{\rm NP}(b)$ in the resummed Drell-Yan spectra [24,25].

Actually, this finding should not be too surprising because for a typical Drell-Yan pair of $Q\sim 5$ GeV and $q_T \sim 1$ GeV at fixed target energies, the ratio Q^2/q_T^2 is about 25, which is much smaller than the 8×10^3 for a Z^0 production at the collider energies. On the other hand, when Q^2 is much larger than the typical q_T^2, the q_T spectrum in this region has an enhanced peak at a finite value of q_T and a slower fall off in comparison with the Gaussian-like distribution, as sketched in Fig. 1. The size of the enhancement and the size of the region depend on the value of Q and the range of q_T [25]. Furthermore, because of the slower fall of the transverse momentum distribution with a full resummation of the large logarithms at low q_T, the transition between the resummed distribution and the large q_T distribution calculated in the fixed order perturbative QCD should be smoother than the unphysical kink, as shown in Fig. 2, at the point where the Gaussian-like distributions are matched with the large q_T perturbative tails. Since we concentrate on Drell-Yan q_T spectrum at fixed target energies in this paper, we will effectively merge regions (I) and (II) in the rest of our discussions.

The large q_T region, labeled by III in Fig. 1, corresponds to the region where $q_T > q_T^L$. In this region, the transverse momentum spectrum calculated in conventional fixed order perturbative QCD should be reliable [28,29], as shown by the solid line in Fig. 1. This perturbative tail of q_T spectrum has a typical powerlike behavior.

In conclusion, the Drell-Yan q_T spectrum at fixed target energies can be represented by a Gaussian-like distribution in the small q_T region and a perturbatively calculated tail in the large q_T region

$$\frac{d\sigma}{dQ^2\,dq_T^2}=\frac{d\sigma^{(\rm I)}}{dQ^2\,dq_T^2}\,\theta(q_T^L-q_T)+\frac{d\sigma^{(\rm III)}}{dQ^2\,dq_T^2}\,\theta(q_T-q_T^L)$$
$$=\frac{d\sigma^{(\rm I)}}{dQ^2\,dq_T^2}+\left(\frac{d\sigma^{(\rm III)}}{dQ^2\,dq_T^2}-\frac{d\sigma^{(\rm I)}}{dQ^2\,dq_T^2}\right)\theta(q_T-q_T^L), \tag{5}$$

where $d\sigma^{(\rm III)}/dQ^2\,dq_T^2$ is the perturbatively calculated q_T spectrum [28,29], which is valid for region (III), and $d\sigma^{(\rm I)}/dQ^2\,dq_T^2$ is the Gaussian-like distribution defined in Eq. (3), which is able to fit data in regions (I)+(II). Since $d\sigma^{(\rm III)}/dQ^2\,dq_T^2$ is calculable, q_T^L and parameters $N_{\rm DY}$ and τ in Eq. (3) are the only unknowns for the Drell-Yan q_T spectrum at fixed target energies.

Taking the moments of the Drell-Yan q_T spectrum in Eq. (5), we can express the parameters $N_{\rm DY}$ and τ in Eq. (3) in terms of physically measurable quantities. For example, by integrating the q_T spectrum in Eq. (5), we obtain the Drell-Yan total cross section as the zeroth moment of the q_T spectrum. Using the data shown in Fig. 2, we found that the contribution from the second term in Eq. (5) $\int_{q_T^L}(d\sigma^{(\rm III)}/dQ^2\,dq_T^2-d\sigma^{(\rm I)}/dQ^2\,dq_T^2)dq_T^2$ is much less than one percent of the contribution from the first term $\int(d\sigma^{(\rm I)}/dQ^2\,dq_T^2)dq_T^2$. Therefore, up to the less than one percent uncertainty, we obtain the normalization $N_{\rm DY}$ in Eq. (3) as

$$N_{\rm DY}\approx\frac{d\sigma}{dQ^2}. \tag{6}$$

Define the Drell-Yan averaged transverse momentum square as

$$\langle q_T^2\rangle\equiv\frac{\int q_T^2(d\sigma/dQ^2\,dq_T^2)dq_T^2}{d\sigma/dQ^2}. \tag{7}$$

Substituting Eqs. (5) and (6) into our definition in Eq. (7), we obtain

$$\langle q_T^2\rangle=2\tau^2+\Gamma(q_T^L,\tau^2), \tag{8}$$

with

$$\Gamma(q_T^L,\tau^2)\equiv\frac{1}{d\sigma/dQ^2}\int_{q_T^L}q_T^2\left(\frac{d\sigma^{(\rm III)}}{dQ^2\,dq_T^2}-\frac{d\sigma^{(\rm I)}}{dQ^2\,dq_T^2}\right)dq_T^2. \tag{9}$$

In principle, $\Gamma(q_T^L,\tau^2)$ is calculable, and its τ^2 dependence is from the $d\sigma^{(I)}/dQ^2dq_T^2$. Even though $\langle q_T^2\rangle$ enhances the contributions from the perturbative tail, we find that the $\Gamma(q_T^L,\tau^2)$ in Eq. (8) is much less than ten percent of the first term for the data in Fig. 2 at fixed target energies. Therefore, by iteration, we derive the width of the Gaussian-like distribution $d\sigma^{(\rm I)}/dQ^2dq_T^2$ in Eq. (3) as

$$2\tau^2 \approx \langle q_T^2\rangle - \Gamma(q_T^L, \tau^2 = \langle q_T^2\rangle/2), \tag{10}$$

where the precise value of q_T^L will be determined later.

Substituting Eqs. (6) and (8) into Eq. (3), we obtain the Drell-Yan q_T spectrum at small q_T in hadron-nucleon collisions as

$$\frac{d\sigma_{\rm DY}^{hN}}{dQ^2\, dq_T^2} = \frac{d\sigma_{\rm DY}^{hN}}{dQ^2} \frac{1}{\langle q_T^2\rangle_{\rm DY}^{hN} - \Gamma(q_T^L)_{\rm DY}^{hN}} e^{-q_T^2/[\langle q_T^2\rangle_{\rm DY}^{hN} - \Gamma(q_T^L)_{\rm DY}^{hN}]}, \tag{11}$$

where the superscript hN represents the hadron-nucleon collisions, $\langle q_T^2\rangle_{\rm DY}^{hN}$ is the averaged transverse momentum square for the Drell-Yan production in hadron-nucleon collisions, and the short-handed notation $\Gamma(q_T^L)_{\rm DY}^{hN} \equiv \Gamma(q_T^L, \tau^2 = \langle q_T^2\rangle_{\rm DY}^{hN}/2)_{\rm DY}^{hN}$ with $\Gamma(q_T^L, \tau^2)$ defined in Eq. (9). We emphasize that all quantities, $d\sigma^{hN}/dQ^2$, $\langle q_T^2\rangle_{\rm DY}^{hN}$, and $\Gamma(q_T^L)_{\rm DY}^{hN}$, which completely define the Drell-Yan q_T spectrum in the small q_T region, are either independently measurable or perturbatively calculable. For the Drell-Yan data in Fig. 2 at fixed target energies, we found that $\langle q_T^2\rangle_{\rm DY}^{hN}$ ranges from 1.5 to 1.8 GeV^2, and $\Gamma(q_T^L)_{\rm DY}^{hN}$ is less or about ten percent depending on the value of q_T^L.

In order to derive an expression for the nuclear dependence coefficient $\alpha(A,q_T)$, we need to know the Drell-Yan transverse momentum spectrum in hadron-nucleus collisions. In hadron-nucleus collision, initial-state partons have much larger probability to have multiple scattering before the hard collision to produce the Drell-Yan pair. Therefore, in order to obtain the transverse momentum spectrum in hadron-nucleus collisions, we need to consider contributions from both the single scattering and the multiple scattering. For the single scattering contribution to the transverse momentum spectrum in hadron-nucleus collisions, we can use the same arguments given above for the spectrum in hadron-nucleon collisions. Therefore, at fixed target energies, the *single* scattering contribution to $d\sigma^{hA}/dQ^2\, dq_T^2$ in the small q_T region can be well represented by a Gaussian-like distribution.

For the Drell-Yan production, parton initial-state interactions dominate the multiple scattering because the virtual photon does not interact strongly. The initial-state multiple scattering can provide extra transverse momentum to a parton participating the hard collision, and consequently change the transverse momentum spectrum of the produced Drell-Yan pair. Therefore, multiple scattering leads to a broadening in the averaged transverse momentum square $\langle q_T^2\rangle^{hA}$, which is defined in Eq. (7) with the superscript hA representing the hadron-nucleus collisions. Define

$$\Delta\langle q_T^2\rangle \equiv \langle q_T^2\rangle^{hA} - \langle q_T^2\rangle^{hN}, \tag{12}$$

and $\Delta\langle q_T^2\rangle$ is often called the nuclear broadening of the averaged transverse momentum square. It was demonstrated in Refs. [20,30] that the nuclear broadening $\Delta\langle q_T^2\rangle$ is calculable within QCD perturbation theory. In terms of the double scattering and the generalized factorization theorem [15], the transverse momentum broadening for the Drell-Yan pairs $\Delta\langle q_T^2\rangle_{\rm DY}$ was calculated at the leading order in α_s, and was expressed in terms of the quark-gluon correlation functions inside a nucleus [20]:

$$\Delta\langle q_T^2\rangle_{\rm DY} = \left(\frac{4\pi^2\alpha_s}{3}\right) \cdot \frac{\sum_q e_q^2 \int dx'\, \phi_{q/h}^-(x') T_{qg}^{\rm SH}(Q^2/sx')/x'}{\sum_q e_q^2 \int dx'\, \phi_{q/h}^-(x') \phi_{q/A}(Q^2/sx')/x'}, \tag{13}$$

where Σ_q runs over all quark and antiquark flavors, e_q is the fractional charge of quark and antiquark of flavor q, and α_s is the strong coupling constant. In Eq. (13), the $s=(p+p')^2$ with p' the four momentum of the incident hadron and p the averaged momentum per nucleon for the nucleus, and $\phi_{q/h}^-$ and $\phi_{q/A}$ are parton distributions of the hadron and the nucleus, respectively. The $T_{qg}^{\rm SH}(x)$ of flavor q in Eq. (13) is the ''soft-hard'' quark-gluon correlation function in a nucleus and is defined by [10,20]

$$T_{qg}^{\rm SH}(x) = \int \frac{dy^-}{2\pi} e^{ixp^+y^-} \int \frac{dy_1^- dy_2^-}{2\pi} \theta(y^- - y_1^-) \times \theta(-y_2^-) \frac{1}{2} \langle P_A | F_\alpha{}^+(y_2^-) \overline{\psi}_q(0) \times \gamma^+ \psi_q(y^-) F^{+\alpha}(y_1^-) | P_A\rangle, \tag{14}$$

where we assumed that the nucleus is moving along the $+z$ direction, and the superscripts $+$ and $-$ represent the normal $+$ and $-$ components in a light-cone coordinate, respectively. In Eq. (14), the y, y_1, and y_2 represent the position coordinates of the quark and gluon field operators. Although these quark-gluon correlation functions are nonperturbative and unknown, they are universal and as fundamental as the well-known parton distributions [16]. They appear not only in Eq. (13) for the nuclear broadening $\Delta\langle q_T^2\rangle_{\rm DY}$, but also in the nuclear dependence of the Drell-Yan q_T spectrum in hadron-nucleus collisions in the large q_T region [11,12]. In principle, by using the nuclear dependence of the Drell-Yan q_T spectrum in the large q_T region, we can extract these quark-gluon correlation functions and predict the nuclear broadening $\Delta\langle q_T^2\rangle_{\rm DY}$, or vise versa.

On the other hand, by comparing the operator definitions of the quark-gluon correlation functions $T_{qg}^{\rm SH}(x)$, defined in Eq. (14), with the definitions of normalized quark distributions

$$q^A(x) \equiv \frac{1}{A}\phi_{q/A}(x) = \frac{1}{A}\int \frac{dy^-}{2\pi} e^{ixp^+y^-} \left\langle P_A \left| \overline{\psi}_q(0) \frac{\gamma^+}{2} \psi_q(y^-) \right| P_A \right\rangle, \tag{15}$$

one finds that the only difference between the $T_{qg}^{\rm SH}(x)$ and $q^A(x)$ is an operator factor,

$$\int \frac{dy_1^- dy_2^-}{2\pi}\theta(y^- - y_1^-)\theta(-y_2^-)F_\alpha{}^+(y_2^-)F^{+\alpha}(y_1^-).$$

If these two gluon field strength F's are close together in a color singlet nucleon in a normal color confined nuclear target, which limits the $\int dy_1^-$ (or $\int dy_2^-$) to a nucleon size, the extra integration $\int dy_2^-$ (or $\int dy_1^-$) can be extended to the nuclear size to give an extra $A^{1/3}$ factor to the $T_{qg}^{\rm SH}(x)$ over $q^A(x)$. Therefore, one can estimate the size of the quark-gluon correlation functions by modeling them as [10,16]

$$T_{qg}^{\rm SH}(x) = \lambda^2 A^{4/3} q^A(x), \tag{16}$$

where λ is a universal parameter proportional to the averaged color field strength square in position space in a normal nuclear target, and the $q^A(x)$ are the effective nuclear quark distributions normalized by the atomic weight A. With this model for $T_{qg}^{\rm SH}$, the Drell-Yan transverse momentum broadening $\Delta\langle q_T^2\rangle_{\rm DY}$ can be expressed as [20]

$$\Delta\langle q_T^2\rangle_{\rm DY} = \left(\frac{4\pi^2\alpha_s}{3}\right)\lambda^2 A^{1/3} \equiv b_{\rm DY} A^{1/3}. \tag{17}$$

The factor of $A^{1/3}$ in Eq. (17) is an unique feature of parton double scattering in a normal nuclear matter [16]. Data for the transverse momentum broadening is consistent with the features of double scattering [4,20].

Same as the single scattering case, double scattering contributions to the Drell-Yan q_T spectrum in the small q_T region is also dominated by the intrinsic transverse momenta of scattering partons. Similar to Eq. (2), at the leading order in perturbation theory, the *double* scattering contributions to the Drell-Yan $d\sigma^{hA}/dQ^2\,dq_T^2$ can be described by [20]

$$\frac{d\sigma_D^{hA}}{dQ^2\,d^2q_T} \propto T_{qg}(x,x_1,x_2,k_T)\,\delta^2(\vec{q}_T - \vec{k}_T), \tag{18}$$

where the subscript D indicates the double scattering, and the proportionality coefficient depends on the structure of partonic double scattering. In Eq. (18), $\vec{q}_T$ is the transverse momentum vector of the observed Drell-Yan pair, $\vec{k}_T$ represents the intrinsic transverse momentum vector of the gluon which gives additional scattering, and $T_{qg}(x,x_1,x_2,k_T)$ represents a general quark-gluon correlation function with x, x_1, and x_2 being the light-cone momentum fractions carried by the quark and gluon fields, and k_T is the magnitude of $\vec{k}_T$ [16,20]. Integrations over parton momenta $dxdx_1dx_2$ reduce the general $T_{qg}(x,x_1,x_2,k_T)$ to either $T_{qg}^{\rm SH}$, defined in Eq. (14), or $T_{qg}^{\rm DH}$ which is defined later in Eq. (25), depending on the structure of the partonic part of the double scattering. Similar to Eq. (3), we can broaden the δ function in Eq. (18) by its Gaussian-representation to include the effect of intrinsic transverse momentum of incoming quark or antiquark. We can also take into account the effect of gluon's intrinsic transverse momentum by using a Gaussian-like distribution for the k_T dependence of the T_{qg}. After integrating over the intrinsic k_T dependence, we find that just like the single scattering case, the double scattering contributions to the Drell-Yan q_T spectrum in the small q_T region can also be expressed in terms of a Gaussian-like distribution defined in Eq. (3) with a broadened width.

In order to understand the Drell-Yan q_T spectrum in the region (II) in hadron-nucleus collisions, in principle, we have to carry out the resummation of the large logarithms at the presence of multiple scattering. Following the generalized factorization theorem [15], the resummation of the large logarithms at the presence of factorizable partonic multiple scattering can be carried out by using renormalization group method. In order to resum the large logarithms due to gluon radiations, it is necessary to calculate anomalous dimensions of the multiparton correlation functions for deriving the kernel of the renormalization group equation. However, following the same arguments given above for the single scattering case, the resummed Drell-Yan q_T spectrum in region (II) at the fixed target energies is mainly determined by the nonperturbative input distribution $F^{\rm NP}(b)$, which generalizes the perturbatively resummed Drell-Yan b-space distribution to the nonperturbative large b regime in order to perform the Fourier transform back to the q_T space. As argued above, the Drell-Yan q_T spectrum at the presence of multiple scattering should still have a Gaussian-like distribution in the small q_T region, and we expect that the nonperturbative $F^{\rm NP}(b)$ at the presence of multiple scattering should also have a Gaussian-like distribution. Therefore, at the fixed target energies, we can merge the region (I) and (II) of the Drell-Yan q_T spectrum in hadron-nucleus collisions. Since we limit this paper to test the consistency of QCD treatment of multiple scattering at fixed target energies, which has not been done, we will defer a complete analysis of QCD resummation at the presence of multiple scattering to a future publication, which will be very important for the nuclear dependence of Drell-Yan q_T spectrum at the collider energies.

Similar to the case in hadron-nucleon scatterings, when $q_T > q_T^L$, the Drell-Yan q_T spectrum should have a perturbatively calculable tail in region (III), and its nuclear dependences are perturbatively calculable and were calculated in Ref. [11]. Therefore, the Drell-Yan q_T spectrum in hadron-nucleus collisions should have the same form as that in Eq. (5). Using the calculated perturbative tail for the Drell-Yan spectrum in hadron-nucleus collisions, we find that similar to the hadron-nucleon case, the second term in Eq. (5) contributes only about one percent of the total cross section $d\sigma^{hA}/dQ^2$. Therefore, similar to Eq. (6), we can identify the normalization factor of the Gaussian-like distribution to be the total cross section $d\sigma^{hA}/dQ^2$.

Similar to Eq. (11), we derive the Drell-Yan transverse momentum spectrum at small q_T in hadron-nucleus collisions as

$$\frac{d\sigma^{hA}}{dQ^2\,dq_T^2} = \frac{d\sigma^{hA}}{dQ^2}\,\frac{1}{\langle q_T^2\rangle_{\rm DY}^{hA} - \Gamma(q_T^L)_{\rm DY}^{hA}}\,{\rm e}^{-q_T^2/(\langle q_T^2\rangle_{\rm DY}^{hA} - \Gamma(q_T^L)_{\rm DY}^{hA})}, \tag{19}$$

where the superscript hA represents the hadron-nucleus col-

lisions, $\langle q_T^2\rangle_{\rm DY}^{hA}=\langle q_T^2\rangle_{\rm DY}^{hN}+\Delta\langle q_T^2\rangle_{\rm DY}$, and the nuclear broadening $\Delta\langle q_T^2\rangle_{\rm DY}$ is given in Eq. (13) or Eq. (17). In Eq. (19), $\Gamma(q_T^L)_{\rm DY}^{hA}\equiv\Gamma(q_T^L,\tau^2=\langle q_T^2\rangle_{\rm DY}^{hA}/2)_{\rm DY}^{hA}$ with $\Gamma(q_T^L,\tau^2)_{\rm DY}^{hA}$ defined in Eq. (9) with the calculable hadron-nucleon q_T spectrum replaced by the corresponding hadron-nucleus q_T spectrum. Similar to the hadron-nucleon case, we find that the $\Gamma(q_T^L)_{\rm DY}^{hA}$ in Eq. (19) is much smaller than corresponding $\langle q_T^2\rangle_{\rm DY}^{hA}$. Since the Drell-Yan total cross section $d\sigma^{hA}/dQ^2$ has almost no nuclear dependence, Eq. (19) shows that the nuclear broadening $\Delta\langle q_T^2\rangle_{\rm DY}$ determines the Drell-Yan q_T spectrum at small q_T in hadron-nucleus collisions. From Eqs. (11) and (19), we can derive the nuclear dependence coefficient $\alpha(A,q_T)$ for the Drell-Yan process in small q_T region.

III. THE NUCLEAR DEPENDENCE COEFFICIENT FOR THE DRELL-YAN PRODUCTION

In this section, we derive the nuclear dependence coefficient $\alpha(A,q_T)$ for the Drell-Yan production in the small q_T region. We also show that the derived $\alpha(A,q_T)$ in the small q_T region is naturally connected to the perturbatively calculated $\alpha(A,q_T)$ in the large q_T region.

Substituting Eqs. (11) and (19) into Eq. (1), we derive the $\alpha_{\rm DY}(A,q_T)$ for the Drell-Yan production in the small q_T region

$$\alpha_{\rm DY}(A,q_T)=1+\frac{1}{\ln(A)}\left[\ln[R_{\rm DY}^A(Q^2)]+\ln\left(\frac{1}{1+\chi_{\rm DY}}\right)+\frac{\chi_{\rm DY}}{1+\chi_{\rm DY}}\frac{q_T^2}{\langle q_T^2\rangle_{\rm DY}^{hN}-\Gamma(q_T^L)_{\rm DY}^{hN}}\right], \tag{20}$$

where $R_{\rm DY}^A(Q^2)\equiv(1/A)(d\sigma^{hA}/dQ^2)/(d\sigma^{hN}/dQ^2)$. The $\chi_{\rm DY}$ in Eq. (20) is defined by

$$\chi_{\rm DY}\equiv\frac{\Delta\langle q_T^2\rangle_{\rm DY}-\Delta\Gamma(q_T^L)_{\rm DY}}{\langle q_T^2\rangle_{\rm DY}^{hN}-\Gamma(q_T^L)_{\rm DY}^{hN}}\approx\frac{\Delta\langle q_T^2\rangle_{\rm DY}}{\langle q_T^2\rangle_{\rm DY}^{hN}}, \tag{21}$$

with $\Delta\langle q_T^2\rangle_{\rm DY}$ given in Eq. (17), and $\Delta\Gamma(q_T^L)_{\rm DY}\equiv\Gamma(q_T^L)_{\rm DY}^{hA}-\Gamma(q_T^L)_{\rm DY}^{hN}$. Because $\Gamma(q_T^L)_{\rm DY}$ contributes less than ten percent to $\langle q_T^2\rangle_{\rm DY}$ in both hadron-nucleon and hadron-nucleus collisions, $\Delta\Gamma(q_T^L)_{\rm DY}$ is also much smaller than $\Delta\langle q_T^2\rangle_{\rm DY}$. Since the $\chi_{\rm DY}$ and $\langle q_T^2\rangle_{\rm DY}^{hN}$ have no dependence on q_T, the nuclear dependence coefficient $\alpha_{\rm DY}(A,q_T)$ in Eq. (20) for the Drell-Yan production in the small q_T region shows an universal quadratic dependence on q_T: $\alpha_{\rm DY}(A,q_T)=a_1+b_1q_T^2$. The parameters a_1 and b_1 are completely determined by either perturbatively calculable quantities [such as $\Delta\langle q_T^2\rangle$ and the $\Gamma(q_T^L)$'s] or independently measurable quantities [such as $R_{\rm DY}^A(Q^2)$ and $\langle q_T^2\rangle^{hN}$].

Using E772 [4] and NA10 [3] data on $\Delta\langle q_T^2\rangle_{\rm DY}$ and Eq. (17), we obtain that $\Delta\langle q_T^2\rangle_{\rm DY}\sim 0.022A^{1/3}$ GeV^2, which is between 0.05 and 0.13 GeV^2 for all practical nuclear targets. On the other hand, the value of $\langle q_T^2\rangle^{hN}$ for the data in Fig. 2 is ranging from 1.5 to 1.8 GeV^2. Therefore, the $\chi_{\rm DY}$ defined in Eq. (21) should be a small number.

Substituting Eqs. (17) and (21) into Eq. (20), and taking the small $\chi_{\rm DY}$ limit, we obtain

$$\alpha_{\rm DY}(A,q_T)\approx 1+\frac{\chi_{\rm DY}}{\ln(A)}\left[-1+\frac{q_T^2}{\langle q_T^2\rangle_{\rm DY}^{hN}-\Gamma(q_T^L)_{\rm DY}^{hN}}\right]+O\left(\frac{\chi_{\rm DY}^2}{\ln(A)}\right)\approx 1+\frac{b_{\rm DY}}{\langle q_T^2\rangle_{\rm DY}^{hN}}\left[-1+\frac{q_T^2}{\langle q_T^2\rangle_{\rm DY}^{hN}}\right], \tag{22}$$

where $b_{\rm DY}=(4\pi^2\alpha_s/3)\lambda^2$ is defined in Eq. (17). Here we used the experimental fact that $R_{\rm DY}^A(Q^2)\approx 1$. In deriving the second line in Eq. (22), we used $A^{1/3}\sim\ln(A)$, which is a good approximation for most relevant targets, and we neglected the small $\Gamma(q_T^L)_{\rm DY}^{hN}$. For a given beam energy, $\langle q_T^2\rangle_{\rm DY}^{hN}$ for the Drell-Yan pairs has a very weak dependence on Q and no dependence on A. Therefore, Eq. (22) shows that the leading contribution to the $\alpha_{\rm DY}(A,q_T)$ for the Drell-Yan production is a function of q_T and independent of A in the small q_T region.

From the size of the correction term in Eq. (22), it is clear that the $\alpha_{\rm DY}(A,q_T)$ for the Drell-Yan production is insensitive to the atomic weight A of targets. Furthermore, from Eq. (20), we obtain

$$\alpha_{\rm DY}(q_T=0)\approx 1-\frac{\ln(1+\chi_{\rm DY})}{\ln(A)}\approx 1-\frac{\chi_{\rm DY}}{\ln(A)}\approx 1-\left(\frac{4\pi^2\alpha_s}{3}\right)\frac{\lambda^2}{\langle q_T^2\rangle_{\rm DY}^{hN}}. \tag{23}$$

From Eqs. (21) and (23), it is clear that $\alpha_{\rm DY}(q_T=0)$ is determined by the nuclear broadening $\Delta\langle q_T^2\rangle_{\rm DY}$. If there is nuclear broadening in averaged transverse momentum square (i.e., $\chi_{\rm DY}>0$), the transverse momentum spectrum is suppressed at $q_T\sim 0$. For a normal nuclear target, the amount of the suppression at $q_T\sim 0$ is insensitive to the atomic number A of targets.

Equation (20) shows that as q_T increases $\alpha_{\rm DY}(A,q_T)$ increases as well, and it changes from less than 1 to a value larger than 1. Let q_T^c correspond to the critical value of q_T at which $\alpha_{\rm DY}(A,q_T^c)=1$, and we have

$$(q_T^c)^2\approx\langle q_T^2\rangle_{\rm DY}^{hN}\left[\frac{1+\chi_{\rm DY}}{\chi_{\rm DY}}\right]\ln(1+\chi_{\rm DY})\approx\langle q_T^2\rangle_{\rm DY}^{hN}[1+O(\chi_{\rm DY})]. \tag{24}$$

Similar to $\alpha_{\rm DY}(A,q_T=0)$, the q_T^c in Eq. (24) has a very weak dependence on the atomic number A for a normal nuclear target.

In the rest of this section, we show that the $\alpha_{\rm DY}(A,q_T)$ in Eq. (20) [or approximately in Eq. (22)] for the small q_T

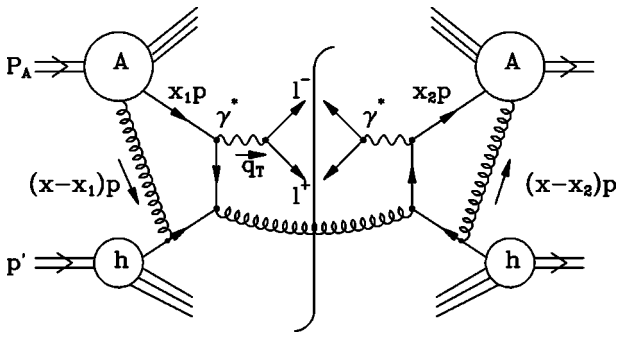

FIG. 3. Sample Feynman diagram for the double scattering contributions to the nuclear dependence of the Drell-Yan q_T spectrum at large q_T.

region is naturally connected to the perturbatively calculated $\alpha_{\rm DY}(A,q_T)$ in the large q_T region [11].

The nuclear dependence of the Drell-Yan transverse momentum spectrum in the large q_T region can be calculated in QCD perturbation theory [11,12]. The ratio of the Drell-Yan q_T spectrum $R(A,q_T)=A^{\alpha(A,q_T)-1}$ defined in Eq. (1) was derived in Ref. [11] for the large q_T region. It was found [11] that at the leading order in α_s, the $R(A,q_T)$ depends on two types of parton correlation functions due to different structure of partonic double scattering. For example, consider a double scattering Feynman diagram in Fig. 3, which contributes to the nuclear dependence of the Drell-Yan q_T spectrum in the large q_T region. In Fig. 3, x, x_1, and x_2 are independent parton momentum fractions for the double scattering. For the contour integration of dx_i's, taking the residues of poles of the partonic double scattering diagram can eliminate the oscillation factor $e^{-x_i p^+ y_i^-}$ for corresponding integrations dy_i^-'s in position space [10,11]. The lack of the oscillation factor for integration of position variable y_i^-'s leads to an $A^{1/3}$-type (or nuclear size) dependence. The partonic double scattering diagram in Fig. 3 has two types of poles: one type that corresponds to $x-x_1\to 0$ and $x-x_2\to 0$, and the other type that corresponds to $x_1=x_2\equiv x_a$ and $x-x_1=x-x_2\equiv x_b$ with both x_a and x_b finite. The first type poles lead to the so-called ''soft-hard'' quark-gluon correlation functions defined in Eq. (14), which have both dy_1^- and dy_2^- integrations free of the oscillation factor. The second type poles lead to the so-called ''double-hard'' quark-gluon correlation functions [10,11]

$$T_{qg}^{\rm DH}(x_a,x_b)=\frac{1}{x_b p^+}\int\frac{dy_1^-}{2\pi}\int\frac{dy^-}{4\pi}\int p^+ dy_2^-\,\theta(y^--y_1^-)\times\theta(-y_2^-)e^{ix_a p^+ y^-}e^{ix_b p^+(y_1^--y_2^-)}\times\langle P_A|F_\sigma{}^+(y_2^-)\bar{\psi}_q(0)\gamma^+\psi_q(y^-)\times F^{+\sigma}(y_1^-)|P_A\rangle, \tag{25}$$

where all the variables and the superscripts carry the same meaning as those in Eq. (14). Unlike the soft-hard correlation functions, only one dy_2^- (or dy_1^-) integration in the double-hard correlation functions defined in Eq. (25) is free of the oscillation factor. But, this dy_2^- (or dy_1^-) integration is just enough to produce an $A^{1/3}$-type enhancement to the Drell-Yan q_T spectrum [10,11]. In addition to the double-hard quark-gluon correlation functions, the nuclear dependence at large q_T also receives contributions from quark-quark and gluon-gluon correlation functions [11]. By comparing the operator definitions of the normal quark and gluon distributions with the operator definitions for the double-hard correlation functions, similar to Eq. (16), the double-hard quark-gluon correlation functions can be parametrized as [31]

$$T_{qg}^{\rm DH}(x_a,x_b)=(2\pi C)A^{4/3}q^A(x_a)G^A(x_b), \tag{26}$$

with $q^A(x_a)$ and $G^A(x_b)$ the effective nuclear parton distributions normalized by the atomic number A. The constant parameter C represents the size of quantum interference between different nucleon states and possible overlap of two nucleon parton distributions in a nucleus. Currently, there is no direct observable yet to extract information on $T^{\rm DH}$ [12] or to determine the parameter C in Eq. (26).

When x_1 (or x_2) goes to zero, the corresponding parton fields reach the saturation region, and the $T^{\rm DH}$ is reduced to $T^{\rm SH}$. Therefore, if we assume the full quantum interference (in saturation region), the proportionality constant C in Eq. (26) can be related to the λ^2 in Eq. (16) by using the following identity:

$$\lim_{x_b\to 0} x_b T_{qg}^{\rm DH}(x_a,x_b)=T_{qg}^{\rm SH}(x_a). \tag{27}$$

From Eq. (27) and the definitions of $T_{qg}^{\rm DH}$ and $T_{qg}^{\rm SH}$, we obtain

$$C\approx\frac{\lambda^2}{2\pi x G(x)|_{x\approx 0}}, \tag{28}$$

where $xG(x)|_{x\approx 0}$ is the gluon momentum density at $x\to 0$ limit, which is believed to be of order 1 at low energy [32,33]. The precise value of $xG(x)|_{x\approx 0}$ depends on the physics of parton saturation [33], and it has not been well measured experimentally. In this paper, we choose $xG(x)|_{x\approx 0}\approx 3$ based on the simple form $G(x)\approx 3x^{-1}(1-x)^5$, which is a result of a simple power counting for gluons at large x, Regge behavior for gluons at small x, and an assumption that gluons carry 50% momentum of the beam hadron. A different choice for $xG(x)|_{x\approx 0}$ results in a different overall normalization factor C. The λ^2 in Eq. (28) is the same as the one in Eq. (16) for the soft-hard quark-gluon correlation functions. Other correlation functions can also be determined in a similar way. Therefore, the λ^2 becomes the only parameter to fix the normalization of both the soft-hard $T^{\rm SH}$ and the double-hard $T^{\rm DH}$ correlation functions. If we extract the value of λ^2 from the data on the transverse momentum broadening $\Delta\langle q_T^2\rangle_{\rm DY}$ by using Eq. (17), we can fix our predictions of the nuclear dependence for the Drell-Yan q_T spectrum in the large q_T region.

On the other hand, by assuming that the quantum interference between parton field operators from different nucleon states are strongly suppressed, one derives

$$C=0.35/(8\pi r_0^2)\ \ {\rm GeV}^2 \tag{29}$$

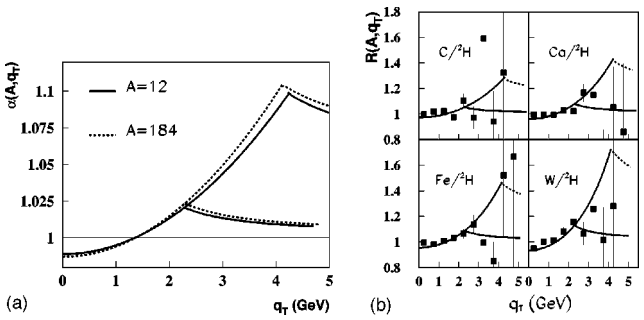

FIG. 4. (a) $\alpha(A,q_T)$ for the Drell-Yan production as a function of q_T. Low q_T region is given by Eq. (20), and high q_T region is given by Ref. [11] with the maximum and minimum values of the C discussed in the text. (b) $R(A,q_T)$ for the Drell-Yan production as a function of q_T. Data from E772 [4,34], and the theory curves are given by $R(A,q_T)=A^{\alpha(A,q_T)-1}$ with $\alpha(A,q_T)$ given in (a).

with $r_0 \approx 1.1-1.25$ fm, which is just a geometric factor for finding two nucleons at the same impact parameter [11,31].

Because of a combination of a small value of the measured λ^2 from Drell-Yan data [3,4] and a choice of $[xG(x)]_{x\approx 0}\approx 3$, the numerical values of C determined by Eqs. (29) and (28) approximately differ by a factor of 20. We believe that the numerical value for the C given in Eq. (29) without any quantum interference between parton field operators should represent a possible maximum for the C, while the value given in Eq. (28) with full quantum interference (in the saturation region) represents a possible minimum for the C. The parameter C reflects the size of quantum interference involved in the multiparton correlation functions, and its precise value should be between those obtained by Eqs. (29) and (28). More discussions on the consequences of a different value of the C are given in Sec. V.

In Fig. 4, we plot the $\alpha_{\rm DY}(A,q_T)$ as a function of q_T for various nuclear targets. For the small q_T region, we used our $\alpha_{\rm DY}(A,q_T)$ in Eq. (20). For the large q_T region, we used the perturbative calculations of $R(A,q_T)\equiv A^{\alpha(A,q_T)-1}$ in Ref. [11]. In plotting Fig. 4(a), we used $\langle q_T^2\rangle_{\rm DY}^{hN}=1.8$ GeV^2 and $\Delta\langle q_T^2\rangle_{\rm DY}=0.022A^{1/3}$ GeV^2. We choose the value of λ^2 to be consistent with $b_{\rm DY}=0.022$ GeV^2. The solid and dashed lines correspond to the nuclear target C ($A=12$) and W ($A=184$), respectively. For the large q_T region, we plotted the perturbatively calculated $\alpha_{\rm DY}(q_T)$ [11] with the maximum and minimum values of the C discussed above. It is clear from Fig. 4(a) that our nuclear dependence coefficient for the Drell-Yan q_T spectrum in the small q_T region is naturally connected to the perturbatively calculated $\alpha_{\rm DY}(A,q_T)$ in the large q_T region. Without any adjustment of parameters, we choose the q_T^L to be the transverse momentum at the cross point between the low q_T and high q_T spectrum. Without any extra free fitting parameters, our predictions shown in Fig. 4 are consistent with data in small q_T region, and due to the large error in data at high q_T, current Drell-Yan data at the fixed target energies are consistent with almost any value of the C between the maximum and the minimum discussed above. Different value of C resulted in different value of q_T^L at the crossing point. From Fig. 4(a), the value of q_T^L is between $2.3-4.0$ GeV, which is very reasonable.

As expected from Eq. (22), the $\alpha_{\rm DY}(A,q_T)$ in Fig. 4(a) shows very little dependence on the atomic weight A. Therefore, the $\alpha_{\rm DY}(A,q_T)$ for the Drell-Yan production in the small q_T region has scaling on A and shows an universal quadratic dependence on q_T. The scaling violation due to the potential A dependence is extremely small for a normal color confined nuclear target. Since $\langle q_T^2\rangle_{\rm DY}^{hN}$ can depend on the beam energy and Q as well as the scaled longitudinal momentum (x_F), our universal function $\alpha_{\rm DY}(A,q_T)$ in Eq. (20) can depend on these observables accordingly [30].

In Fig. 4(b), we compare our $\alpha_{\rm DY}(A,q_T)$ shown in Fig. 4(a) with data from Fermilab experiment E772 [4,34]. Using the $\alpha_{\rm DY}(A,q_T)$ in Fig. 4(a), we plot the ratio of cross sections $R(A,q_T)=A^{\alpha(A,q_T)-1}$ as a function of q_T. All parameters are the same as those used in plotting Fig. 4(a). Also plotted in Fig. 4(b) are data from E772 on four different nuclear targets: C, Ca, Fe, and W [4,34]. It is very clear that without any extra fitting parameter, our predictions for the nuclear dependence coefficient $\alpha_{\rm DY}(A,q_T)$ provide a good description of the data on $R(A,q_T)$ for all values of q_T. The A dependence in $R(A,q_T)$ in Fig. 4(b) is clearly consistent with the A independence of $\alpha_{\rm DY}(A,q_T)$ shown in Fig. 4(a). Better data can provide even more critical tests of our predictions for $\alpha_{\rm DY}(A,q_T)$.

Figure 4 demonstrates a clear consistency of the generalized QCD factorization theorem [15], which was used to calculate the nuclear broadening $\Delta\langle q_T^2\rangle_{\rm DY}$ and the nuclear dependence in the large q_T region. Even though the nuclear broadening $\Delta\langle q_T^2\rangle_{\rm DY}$ is dominated by information at low q_T while the perturbative tail [or the $\alpha_{\rm DY}(A,q_T)$ in the large q_T region] is controlled by dynamics at large q_T, our derived $\alpha_{\rm DY}(A,q_T)$ for the small q_T region is naturally linked to that for the large q_T region without free fitting parameters. More discussions on the uncertainties, such as the resummation and the choice of the parameter C, will be given in Sec. V.

IV. THE NUCLEAR DEPENDENCE COEFFICIENT FOR J/ψ PRODUCTION

A major difference between the Drell-Yan production and J/ψ production is the final-state interaction. Because of the virtual photon, the Drell-Yan production has only initial-state interactions while J/ψ production has both initial-state and final-state interactions. Therefore, one may conclude that the nuclear dependence of the transverse momentum spectrum for J/ψ and the Drell-Yan production could be different due to the strong final-state interactions. However, we argue in this section that in the small q_T region at fixed target energies, J/ψ transverse momentum spectrum can also be well represented by a Gaussian-like distribution, and the nuclear dependence coefficient $\alpha(A,q_T)$ for J/ψ production is very similar to that for the Drell-Yan production.

Kinematically, hadronic J/ψ production is very much like the Drell-Yan production with $Q\sim M_{J/\psi}$. Therefore, the J/ψ transverse momentum spectrum also has three similar characteristic regions shown in Fig. 1. However, because J/ψ mass $M_{J/\psi}$ is smaller than any typical Q measured from the Drell-Yan continuum, the logarithm $[\alpha_s \ln^2(M_{J/\psi}/q_T^2)]^n$ for

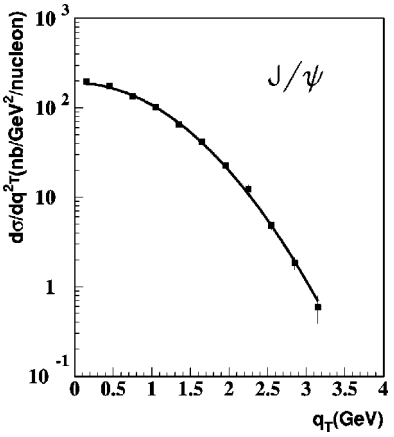

FIG. 5. Fermilab E771 data on J/ψ transverse momentum spectrum [35] in comparison with a fit of Gaussian-like distribution.

J/ψ production should be less important than any Drell-Yan production. We then expect that at fixed target energies, a Gaussian-like distribution can fit J/ψ transverse momentum spectrum at small q_T even better. In Fig. 5, we plot data on J/ψ transverse momentum spectrum from Fermilab experiment E771 [35]. The solid line in Fig. 5 is a fit using a Gaussian-like distribution

$$\frac{d\sigma^{(G)}_{J/\psi}}{dq_T^2} = N_{J/\psi}\frac{1}{2\tau^2}e^{-q_T^2/2\tau^2}, \tag{30}$$

where superscript (G) stands for a Gaussian-like distribution, $N_{J/\psi}$ and τ are the normalization and the width of the Gaussian-like fit, respectively. As expected, the χ^2 for fitting the J/ψ spectrum in Fig. 5 is about 0.9 per degree of freedom, which is much smaller than the χ^2 for fitting Drell-Yan data in Fig. 2, where the χ^2 per degree of freedom is ranging from 1.0 to 2.0.

Similar to Eqs. (2) and (18), at the lowest order in perturbation theory, both the initial-state and final-state double scattering contribution to the J/ψ transverse momentum spectrum in hadron-nucleus collisions is proportional to a δ function $\delta^2(\vec{q}_T-\vec{k}_T)$, where q_T is the total transverse momentum of any produced pre-J/ψ partonic state (e.g., a state of charm and anticharm quark pair), and k_T represents the intrinsic momentum of the gluon which gives additional scattering. Following the same arguments that follows Eq. (18) in Sec. II, we conclude that in the small q_T region, J/ψ transverse momentum spectrum in hadron-nucleus collisions can be well represented by a Gaussian-like distribution shown in Eq. (30), and the normalization $N_{J/\psi}$ and the width τ are given by

$$N_{J/\psi} \approx \sigma^{hA}_{J/\psi},$$
$$2\tau^2 \approx \langle q_T^2\rangle^{hA}_{J/\psi} - \Gamma(q_T^L)^{hA}_{J/\psi}, \tag{31}$$

where $\sigma^{hA}_{J/\psi}$ is the J/ψ total cross section, and $\langle q_T^2\rangle^{hA}_{J/\psi}$ is the averaged transverse momentum square, defined in the same way as that for the Drell-Yan $\langle q_T^2\rangle^{hA}_{DY}$ in Eq. (7). In Eq. (31), $\Gamma(q_T^L)^{hA}_{J/\psi}$ is perturbatively calculable and defined as

$$\Gamma(q_T^L)^{hA}_{J/\psi} \equiv \frac{1}{\sigma^{hA}_{J/\psi}}\int_{q_T^L} q_T^2\left(\frac{d\sigma^{(P)}_{J/\psi}}{dq_T^2} - \frac{d\sigma^{(G)}_{J/\psi}}{dq_T^2}\right)dq_T^2, \tag{32}$$

where $d\sigma^{(P)}_{J/\psi}/dq_T^2$ is a perturbatively calculable q_T spectrum at large q_T, and $d\sigma^{(G)}_{J/\psi}/dq_T^2$ is defined in Eq. (30) with $2\tau^2 = \langle q_T^2\rangle^{hA}_{J/\psi}$. The corresponding transverse momentum spectrum in the small q_T region is given by

$$\frac{d\sigma^{hA}_{J/\psi}}{dq_T^2} = \sigma^{hA}_{J/\psi}\frac{1}{\langle q_T^2\rangle^{hA}_{J/\psi} - \Gamma(q_T^L)^{hA}_{J/\psi}}e^{-q_T^2/[\langle q_T^2\rangle^{hA}_{J/\psi} - \Gamma(q_T^L)^{hA}_{J/\psi}]}. \tag{33}$$

The $\Gamma(q_T^L)^{hA}_{J/\psi}$ is the small contribution to $\langle q_T^2\rangle^{hA}_{J/\psi}$ due to the difference between the perturbative tail and an extended Gaussian-like distribution, and is defined in Eq. (32).

Introduce the nuclear broadening of J/ψ transverse momentum spectrum $\Delta\langle q_T^2\rangle_{J/\psi}$,

$$\Delta\langle q_T^2\rangle_{J/\psi} \equiv \langle q_T^2\rangle^{hA}_{J/\psi} - \langle q_T^2\rangle^{hN}_{J/\psi}, \tag{34}$$

where $\langle q_T^2\rangle^{hN}_{J/\psi}$ is the averaged transverse momentum square of J/ψ production in hadron-nucleon collisions. Similar to Eq. (20), we derive the nuclear dependence coefficient $\alpha(A,q_T)$ for J/ψ production in the small q_T region

$$\alpha_{J/\psi}(A,q_T) = 1 + \frac{1}{\ln(A)}\left[\ln(R^A_{J/\psi}) + \ln\left(\frac{1}{1+\chi_{J/\psi}}\right) + \frac{\chi_{J/\psi}}{1+\chi_{J/\psi}}\frac{q_T^2}{\langle q_T^2\rangle^{hN}_{J/\psi} - \Gamma(q_T^L)^{hN}_{J/\psi}}\right], \tag{35}$$

where $R^A_{J/\psi} \equiv (1/A)\sigma^{hA}_{J/\psi}/\sigma^{hN}_{J/\psi}$, and $\chi_{J/\psi}$ is defined by

$$\chi_{J/\psi} \equiv \frac{\Delta\langle q_T^2\rangle_{J/\psi} - \Delta\Gamma(q_T^L)_{J/\psi}}{\langle q_T^2\rangle^{hN}_{J/\psi} - \Gamma(q_T^L)^{hN}_{J/\psi}} \approx \frac{\Delta\langle q_T^2\rangle_{J/\psi}}{\langle q_T^2\rangle^{hN}_{J/\psi}}. \tag{36}$$

Similar to the Drell-Yan case $\Gamma(q_T^L)^{hN}_{J/\psi}$ and $\Delta\Gamma(q_T^L)_{J/\psi}$ are perturbatively calculable, and much smaller than $\langle q_T^2\rangle^{hN}_{J/\psi}$ and $\Delta\langle q_T^2\rangle_{J/\psi}$, respectively. By comparing Eq. (20) with Eq. (35), we can see that the $\alpha_{J/\psi}(A,q_T)$ for J/ψ production has the same universal quadratic dependence on q_T: $\alpha_{J/\psi}(A,q_T) = a_2 + b_2 q_T^2$, and the parameters a_2 and b_2 are again completely fixed by either perturbatively calculable quantities [such as $\Delta\langle q_T^2\rangle_{J/\psi}$ and $\Gamma(q_T^L)_{J/\psi}$'s] or independently measurable quantities [such as the ratio of the total cross section $(1/A)\sigma^{hA}_{J/\psi}/\sigma^{hN}_{J/\psi}$ and the averaged transverse momentum square $\langle q_T^2\rangle^{hN}_{J/\psi}$].

For hadron-nucleus collisions at fixed target energies, clear nuclear suppression for J/ψ total cross sections has been observed [18,19]. Various theoretical explanations of the observed J/ψ suppression have been proposed [36]. Unlike the virtual photon in the Drell-Yan production, the pro-

duced $c\bar{c}$ are likely to interact with the nuclear medium before they exit. If one assumes each interaction between the $c\bar{c}$ pair and the nuclear medium is about the *same* and can be treated *independently*, one naturally derives the Glauber formula for the suppression

$$R^A_{J/\psi}=\frac{\sigma^{hA}_{J/\psi}/A}{\sigma^{hN}_{J/\psi}}=e^{-\beta L_A}, \tag{37}$$

where β is a parameter characterizing the size of suppression, and $L_A \propto A^{1/3}$ is the effective length of the nuclear medium. In terms of Glauber theory of multiple scattering, the $\beta=\rho_N\sigma_{\rm abs}$ with the nuclear density ρ_N and an effective absorption cross section $\sigma_{\rm abs}$ for breaking a J/ψ meson or for changing a coherent pre-resonance $c\bar{c}$ pair to a pair of open charms. The characteristic feature of the Glauber formula is a straight line on a semi-log plot of $\sigma^{hA}_{J/\psi}$ vs L_A. With a large effective $\sigma_{\rm abs}\sim 6-7$ mb, the Glauber formula given in Eq. (37) fits almost all J/ψ suppression data in hadron-nucleus and nucleus-nucleus collisions [36], except the strong suppression observed in Pb-Pb collisions [19].

If one believes that there is no color-deconfinement or quark-gluon plasma was not formed at present heavy ion collisions at fixed target energies, one has to overcome at least two obvious difficulties of the Glauber formula for the suppression: the size of the effective absorption cross section $\sigma_{\rm abs}$, and the observed nonlinearity of the suppression on the semilog plot of $\sigma^{hA}_{J/\psi}$ vs L_A. It was argued in Ref. [37] that because of the size of the $c\bar{c}$ pair produced in a hard collision, the J/ψ meson has to be formed several fermis later after the production of the $c\bar{c}$ pair. Therefore, the suppression of J/ψ in hadronic collisions should be a result of multiple scattering between the produced $c\bar{c}$ pairs and the nuclear medium before the pairs exit medium [38,39]. Recall the fact that the Glauber formula in Eq. (37) is derived for the propagation of a single particle in a medium. On the other hand, the preresonance J/ψ is a state of at least two particles (e.g., a $c\bar{c}$ pair), and such a two particle state can be changed when it goes through the nuclear medium due to the multiple scattering. Just like the random walk for a pair of particles moving through a medium, multiple scattering increases the relative momentum between the pairs, and therefore, decreases the effective phase space for the pairs to form a bound state J/ψ meson. The observed suppression should be an immediate consequence of the fact that a $c\bar{c}$ pair with a *larger* relative momentum is more likely to become a pair of open charm mesons than a bounded J/ψ. In this picture of J/ψ suppression, the absorption cross section $\sigma_{\rm abs}$ in Eq. (37) is an effective cross section for breaking a $c\bar{c}$ pair of relative momentum $\Delta k_{c\bar{c}}$ into a pair of open charm mesons, and clearly, such an effective cross section depends on the value of $\Delta k_{c\bar{c}}$. The larger $\Delta k_{c\bar{c}}$ is, the larger the effective $\sigma_{\rm abs}$ should be. Because the multiple scattering between gluons and the pair changes the value of $\Delta k_{c\bar{c}}$ while the pair exits the nuclear medium, the effective $\sigma_{\rm abs}$ cannot be a constant, and it should increase as the $c\bar{c}$ passes through the medium. Therefore, we expect a stronger suppression than that predicted by the Glauber formula in Eq. (37) for a large nuclear medium, which results into a non-linear dependendence of the suppression on the semilog plot [38]. The quantitative prediction of the suppression depends on the increase of relative momentum per unit length for the $c\bar{c}$ pairs in nuclear medium. With only two parameters: ε^2, the average relative momentum square per unit length in medium acquired by the $c\bar{c}$ pair and α_F which determines the transition probability for a $c\bar{c}$ pair of relative momentum $\Delta k_{c\bar{c}}$ to form a bound-state J/ψ meson, it was shown in Ref. [38] that this picture of J/ψ suppression is consistent with all existing data including the NA50 data on the total J/ψ cross section as well as its E_T spectrum (or dependence on transverse energy E_T of the J/ψ events).

However, in this paper, we are interested in the general features of the $\alpha_{J/\psi}(A,q_T)$ in hadron-nucleus collisions at fixed target energies. Because of the fact that the ratio of J/ψ total cross sections in *hadron-nucleus* collisions at fixed target energies can be fitted by the Glauber formula in Eq. (37), we will not present any detailed model calculation for the ratio of J/ψ cross sections here [38]. Instead, we will approximate the J/ψ suppression by using the $R^A_{J/\psi}$ defined in Eq. (37) for our discussions in the rest of this paper.

Similar to the Drell-Yan process, the nuclear broadening of transverse momentum square for J/ψ production $\Delta\langle q_T^2\rangle_{J/\psi}$ can be calculated in principle within QCD perturbation theory. In our picture of the J/ψ suppression, the $\Delta\langle q_T^2\rangle_{J/\psi}$ should not be directly tied to the J/ψ suppression, because the broadening is an effect on the total momentum of the $c\bar{c}$ pairs while the suppression is a result of changing the relative momentum of the pairs. This is why the observed nuclear broadening of the transverse momentum square for the J/ψ and Drell-Yan production shows a similar $A^{1/3}$ dependence, while the J/ψ and Drell-Yan total cross sections have a very different suppression.

However, due to extra final-state interactions in J/ψ production and the difference in partonic subprocesses between the Drell-Yan and J/ψ production $\Delta\langle q_T^2\rangle_{J/\psi}$ will depend on the gluon-gluon correlation function in addition to the quark-gluon correlation functions mentioned in previous sections [16]. But, for a normal nuclear target, both these correlation functions should be proportional to the target length or $A^{1/3}$. Similar to Eq. (17), for the normal nuclear targets, we can define

$$\Delta\langle q_T^2\rangle_{J/\psi}=b_{J/\psi}A^{1/3}, \tag{38}$$

where $b_{J/\psi}$ can be extracted from existing data. From Ref. [40], $b_{J/\psi}\approx 0.06$ GeV^2, which is larger than $b_{\rm DY}$. With the averaged transverse momentum square $\langle q_T^2\rangle^{hN}_{J/\psi}\approx 1.68$ GeV^2 extracted from the fit in Fig. 4, we have $\chi_{J/\psi}$ ranges from 0.08 to 0.22 for most relevant nuclear targets. Clearly, $\chi_{J/\psi}$ is larger than $\chi_{\rm DY}$, but, it is still a small number for most targets.

Substituting Eqs. (37) and (38) into Eq. (35), and taking the small $\chi_{J/\psi}$ limit, we derive the leading contribution to the

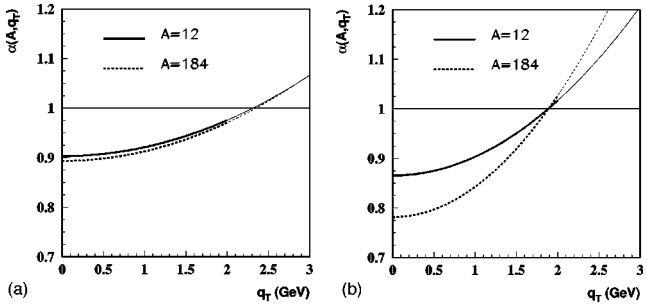

FIG. 6. $\alpha(A,q_T)$ for J/ψ production, defined in Eq. (35), as a function of q_T for normal color confined nuclear targets (a), and for possible color deconfined nuclear medium (b).

$\alpha_{J/\psi}(A,q_T)$ for J/ψ production in a normal nuclear medium as

$$\alpha_{J/\psi}(A,q_T)\approx 1-\beta r_0+\frac{b_{J/\psi}}{\langle q_T^2\rangle_{J/\psi}^{hN}}\left[-1+\frac{q_T^2}{\langle q_T^2\rangle_{J/\psi}^{hN}}\right], \quad (39)$$

where β was introduced in Eq. (37) and r_0 is a proportional constant defined as $L_A=r_0A^{1/3}$. In obtaining Eq. (39), we also neglected the very small $\Gamma(q_T^L)_{J/\psi}^{hN}$. The leading contribution to $\alpha_{J/\psi}(A,q_T)$ given in Eq. (39) has the same universal quadratic dependence on q_T as $\alpha_{\rm DY}(A,q_T)$ in Eq. (22), except a q_T-independent shift in magnitude given by $-\beta[L_A/\ln(A)]$. Since L_A is proportional to $A^{1/3}$ and $A^{1/3}\approx\ln(A)$, the shift in magnitude is insensitive to the atomic number A.

Similar to the Drell-Yan case, we obtain from Eq. (35),

$$\alpha_{J/\psi}(q_T=0)=1-\frac{\ln(1+\chi_{J/\psi})}{\ln(A)}+\frac{1}{\ln(A)}\ln\left(\frac{\sigma_{J/\psi}^{hA}/A}{\sigma_{J/\psi}^{hN}}\right)$$

$$\approx 1-\frac{b_{J/\psi}}{\langle q_T^2\rangle_{J/\psi}^{hN}}-\beta r_0, \quad (40)$$

and it shows that the $\alpha_{J/\psi}(q_T=0)$ is insensitive to the atomic number A for normal nuclear targets. Corresponding to $\alpha_{J/\psi}(q_T^c)=1$, the critical value q_T^c for J/ψ production is given by

$$(q_T^c)^2=\langle q_T^2\rangle_{J/\psi}^{hN}\left(\frac{1+\chi_{J/\psi}}{\chi_{J/\psi}}\right)\left[\ln(1+\chi_{J/\psi})-\ln\left(\frac{\sigma_{J/\psi}^{hA}/A}{\sigma_{J/\psi}^{hN}}\right)\right]$$

$$\approx\langle q_T^2\rangle_{J/\psi}^{hN}\left[1+\frac{\beta r_0}{b_{J/\psi}}\langle q_T^2\rangle_{J/\psi}^{hN}\right], \quad (41)$$

which is again insensitive to the atomic number A.

In Fig. 6, we plot the $\alpha_{J/\psi}(q_T)$, defined in Eq. (35), as a function of q_T for different nuclear targets. In plotting Fig. 6(a), we used $\langle q_T^2\rangle_{J/\psi}^{hN}=1.68$ GeV^2, and $\Delta\langle q_T^2\rangle_{J/\psi}=0.06A^{1/3}$ GeV^2. The solid and dashed lines correspond to the nuclear target C ($A=12$) and W ($A=184$), respectively. As expected from Eq. (39), Fig. 6(a) demonstrates that $\alpha_{J/\psi}(A,q_T)$ for J/ψ production has the same universal functional form as $\alpha_{\rm DY}(A,q_T)$, and it also has scaling on A.

In Fig. 6(a), the thin lines correspond to the large q_T region ($q_T\geqslant 2$ GeV), where we expect that perturbative calculations of the nuclear dependence should be valid. However, such calculations are not available yet.

Since the suppression of J/ψ total cross sections in hadron-nucleus collisions corresponds to a q_T-independent shift in the value of $\alpha_{J/\psi}(A,q_T)$, as we explained earlier, the potential nuclear dependence for the shape of $\alpha_{J/\psi}(A,q_T)$ is most sensitive to the nuclear broadening $\Delta\langle q_T^2\rangle_{J/\psi}$. Although QCD calculation of the nuclear broadening of J/ψ transverse momentum square is not available yet, similar to the Drell-Yan case, we expect the broadening $\Delta\langle q_T^2\rangle_{J/\psi}$ to be proportional to the ''soft-hard'' parton-parton correlation functions. Different from the ''double-hard'' parton-parton correlation functions, both position variables for soft gluons, such as the dy_1^- and dy_2^- in Eq. (14), have no exponential oscillation factors. Therefore, for a color deconfined nuclear medium, both position variables can be as large as the size of the medium; and in principle, the nuclear broadening for J/ψ production can be enhanced as much as $A^{2/3}$, or $\Delta\langle q_T^2\rangle_{J/\psi}\approx bA^{2/3}$, if we let the color correlation length be proportional to $A^{1/3}$. Notice, the proportional parameter b given here is not necessary the same as the $b_{J/\psi}$ extracted from data on a normal nuclear medium. Since we are mainly interested in the A dependence of the $\alpha(A,q_T)$, we will approximate the $b=b_{J/\psi}$ for following discussions.

In a color deconfined medium, the $\chi_{J/\psi}$ in Eq. (35) is no longer a small number, and its $A^{2/3}$ dependence cannot be canceled by the $\ln(A)$. Consequently, the $\alpha_{J/\psi}(A,q_T)$ should become very sensitive to the atomic weight A (or the medium size). In Fig. 6(b), we plotted the $\alpha_{J/\psi}(A,q_T)$ with the same parameters as those used to plot Fig. 6(a), except $\Delta\langle q_T^2\rangle_{J/\psi}=0.06A^{2/3}$ GeV^2, which mimics a color deconfined nuclear medium. Notice that in plotting Fig. 6(b), we did not include a possible change in A dependence of the ratio of J/ψ total cross sections, since it contributes only to a q_T-independent shift in magnitude. From Fig. 6, it is clear that A dependence of the $\alpha_{J/\psi}(q_T)$ for J/ψ production can be a sensitive probe for the color deconfinement of the nuclear medium.

V. DISCUSSIONS AND SUMMARY

In this section, we discuss the predicting power of the nuclear dependence coefficient $\alpha(A,q_T)$ for the Drell-Yan and J/ψ production derived in the previous two sections, and also discuss the uncertainties in the analytical expressions. Finally, we summarize our main conclusions.

The predicting power of the nuclear dependence coefficient $\alpha(A,q_T)$ in Eqs. (20) and (35) is its universal quadratic dependence on q_T, and the fact that all parameters are completely fixed by either calculable or independently measurable quantities: (1) the ratio of *total* cross sections, (2) the averaged transverse momentum square in hadron-*nucleon*

collisions, (3) the nuclear broadening of the averaged transverse momentum square, and (4) the perturbatively calculable $\Gamma(q_T^L)$'s. The ratio of *total* cross sections, σ^{hA}/σ^{hN}, can be either measured in experiments or calculated in a theory. The ratio is independent of q_T, and therefore, it does not affect the shape of $\alpha(A,q_T)$. On the other hand, the averaged transverse momentum square in hadron-*nucleon* collisions, $\langle q_T^2\rangle^{hN}$, does not have any nuclear dependence and can be independently measured. The nuclear broadening of the averaged transverse momentum square, $\Delta\langle q_T^2\rangle$, can be factorized into multiparton correlation functions and perturbatively calculable partonic parts. These nonperturbative multiparton correlation functions are universal and can be extracted from the nuclear dependence in the large q_T region. Therefore, adding the small corrections from the perturbatively calculable $\Gamma(q_T^L)$'s, we can actually predict the $\alpha(A,q_T)$ for the Drell-Yan and J/ψ production. Figure 4(b) is an example of our prediction and its comparison with E772 data.

The main uncertainty in our predictions for $\alpha(A,q_T)$ comes from the size of the QCD resummation for potential large logarithms, such as $[\alpha_s \ln^2(Q^2/q_T^2)]^n$. For the Drell-Yan production at both collider and fixed target energies, our formula for the $\alpha_{\rm DY}(A,q_T)$ should be valid or at least a good approximation, as long as Q^2 is not too large and $q_T \leqslant 2.5$ GeV. For J/ψ production, because $M_{J/\psi}$ is relatively small in comparison with the Q for a typical Drell-Yan pair, our formula for $\alpha_{J/\psi}(A,q_T)$ should be valid for $q_T \leqslant 2$ GeV. When q_T is larger, $\alpha_{J/\psi}(A,q_T)$ should be calculable in perturbative QCD.

Another possible uncertainty in our predictions is the asymptotic value of normal parton distributions as $x\to 0$ at low energy, as seen in Eq. (28). The precise asymptotic value of the parton distributions as $x\to 0$ itself is a very interesting quantity, which can provide rich information on parton saturation [33]. For the quantities we discussed in this paper, different asymptotic values of the parton distributions result into different normalizations of the ''double-hard'' parton-parton correlation functions. Since the contributions from the ''double-hard'' correlation functions to the $\alpha_{\rm DY}(A,q_T)$ in the large q_T region is as important as those from the ''soft-hard'' correlation functions [11], different asymptotic values of the parton distributions can result into a different crossing point between the low q_T spectrum and the high q_T spectrum, and consequently, a slightly different value of the q_T^L. For example, a smaller value of $xG(x)|_{x\sim 0}$ corresponds to a slightly larger value of q_T^L, which actually describes the data slightly better. Although current data are still not sufficient to provide the precise values of parton distributions as $x\to 0$, such asymptotic values can be measured in principle, and corresponding uncertainties can be fixed.

The four key quantities for determining the $\alpha(A,q_T)$: σ^{hA}/σ^{hN}, $\langle q_T^2\rangle^{hN}$, $\Delta\langle q_T^2\rangle$, and $\Gamma(q_T^L)$'s can depend on beam energy, $P_{\rm beam}$, and x_F, and also the value of Q in the case of the Drell-Yan production. For example, the dependence of $\alpha(A,q_T)$ on the beam energy can be qualitatively understood as follows. For given values of x_F (and Q in the case of the Drell-Yan production), a larger $P_{\rm beam}$ (or $\sqrt{S}$) leads to a larger $\langle q_T^2\rangle^{hN}$ because of the larger phase space. From Eq. (23) [or Eq. (40)], we conclude that when $P_{\rm beam}$ increases, the intersection, $\alpha(q_T=0)$, with the vertical axis at $q_T=0$ in Fig. 4 [or Fig. 6(a)] moves closer to one. On the other hand, from Eq. (24) [or Eq. (41)], the increase of the beam energy leads to a larger value of the critical point q_T^c at which the $\alpha(A,q_T^c)=1$. Therefore, the curve of $\alpha(A,q_T)$ becomes flatter when $P_{\rm beam}$ increases, which is consistent with the data from NA10 [41]. Similar qualitative conclusions can be derived for the x_F dependence (or Q dependence in the case of the Drell-Yan production) of $\alpha(A,q_T)$. In any case, one should take into account the possible x_F dependence of all four key quantities that determine $\alpha(A,q_T)$.

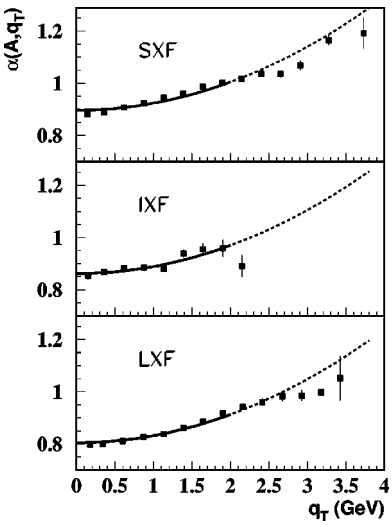

FIG. 7. Comparison of fits, using our universal quadratic form for $\alpha(A,q_T)$ in Eq. (35), with J/ψ data from the Fermilab E866 Collaboration [6] in three regions of different x_F.

Recent data from Fermilab experiment E866 shows that for different regions of x_F, the $\alpha_{J/\psi}(A,q_T)$ for J/ψ production have similar shapes in q_T dependence, but, different magnitudes [6]. It was found that for three x_F regions (small, intermediate, and large), the magnitude of $\alpha_{J/\psi}(A,q_T)$ decreases as x_F increases. This phenomenon is consistent with our prediction of $\alpha_{J/\psi}(A,q_T)$ in Eq. (35) [or Eq. (39)]. According to Eq. (35), the suppression in J/ψ *total* cross sections represents a q_T-independent shift in the magnitude of $\alpha_{J/\psi}(A,q_T)$. The larger the suppression, the smaller $\alpha_{J/\psi}(A,q_T)$. Because of limited x_F range, the ratio of total cross sections $R^A_{J/\psi}\equiv(1/A)\sigma^{hA}_{J/\psi}/\sigma^{hN}_{J/\psi}$ in Eq. (35), becomes x_F dependent. It is an experimental fact that the larger x_F is, the more suppression for J/ψ production (or smaller $R^A_{J/\psi}$) [42]. Therefore, from Eq. (35), the larger x_F, the smaller $\alpha_{J/\psi}(A,q_T)$, which is consistent with experimental data [6]. Although we do not have the four key quantities for different x_F regions to make absolute predictions, we can still test the universality (or consistency) of the $\alpha_{J/\psi}(A,q_T)$ by using the quadratic form in q_T shown in Eq. (35) to fit the data. In Fig. 7, we plot E866 data on $\alpha_{J/\psi}(A,q_T)$ in three separate x_F regions: small (SXF), intermediate (IXF), and large (LXF). We also plot in Fig. 7 our fits to these data with a universal quadratic form in q_T, as shown in Eq. (35). It is clear from Fig. 7 that our universal function for $\alpha_{J/\psi}(q_T)$ is consistent

with all data in the small q_T region, which covers $q_T < q_T^L \sim M_{J/\psi}/2$. Also, as expected, our formula for $\alpha_{J/\psi}(A,q_T)$ deviates from the data when $q_T > M_{J/\psi}/2$. As in the Drell-Yan case, shown in Fig. 4, it will be very interesting to calculate the nuclear dependence of the J/ψ transverse momentum spectrum in the large q_T region to test the QCD dynamics.

In summary, we derived an analytic formula for the nuclear dependence coefficient $\alpha(A,q_T)$ for both the Drell-Yan and J/ψ production in the small q_T region. The formula has a universal quadratic dependence on q_T, and all parameters are completely determined by four key quantities: σ^{hA}/σ^{hN}, $\langle q_T^2 \rangle^{hN}$, $\Delta\langle q_T^2 \rangle$, and $\Gamma(q_T^L)$'s. These quantities can be either calculated in QCD perturbation theory or independently measured in other experiments. We explicitly demonstrated that our $\alpha(A,q_T)$ is consistent with existing data.

Furthermore, we showed that our $\alpha(A,q_T)$ is extremely *insensitive* to the atomic weight A for a normal nuclear target. However, for a color deconfined nuclear medium, the $\alpha(A,q_T)$ becomes strongly dependent on A (or the medium size). Therefore, the A dependence of $\alpha(A,q_T)$ can be a potential observable for detecting a color deconfined system.

ACKNOWLEDGMENTS

We thank M.J. Leitch, J.M. Moss, and J.-C. Peng for helpful communications about experiments and data. This work was supported in part by the U.S. Department of Energy under Grant Nos. DE-FG02-87ER40731 and DE-FG02-96ER40989.

[1] J.W. Cronin *et al.*, Phys. Rev. D **11**, 3105 (1975).
[2] D. Antreasyan *et al.*, Phys. Rev. D **19**, 764 (1979); P.B. Straub *et al.*, Phys. Rev. Lett. **68**, 452 (1992).
[3] NA10 Collaboration, P. Bordalo *et al.*, Phys. Lett. B **193**, 373 (1987).
[4] E772 Collaboration, D. M. Alde *et al.*, Phys. Rev. Lett. **66**, 2285 (1991); **64**, 2479 (1990).
[5] E866 Collaboration, M.A. Vasiliev *et al.*, Phys. Rev. Lett. **83**, 2304 (1999).
[6] E866 Collaboration, M.J. Leitch *et al.*, Phys. Rev. Lett. **84**, 3256 (2000).
[7] NA38 Collaboration, M.C. Abreu *et al.*, Phys. Lett. B **368**, 230 (1996); NA38 Collaboration, C. Baglin *et al.*, *ibid.* **251**, 465 (1990); **368**, 230 (1996).
[8] NA3 Collaboration, J. Badier *et al.*, Z. Phys. C **20**, 101 (1983).
[9] S. Gavin and M. Gyulassy, Phys. Lett. B **214**, 241 (1988); J. Hüfner, Y. Kurihara, and H.J. Pirner, *ibid.* **215**, 218 (1988); J.P. Blaizot and J.-Y. Ollitrault, *ibid.* **217**, 386 (1989); **217**, 392 (1989); D. Kharzeev, M. Nardi, and H. Satz, *ibid.* **405**, 14 (1997).
[10] M. Luo, J.-W. Qiu, and G. Sterman, Phys. Lett. B **279**, 377 (1992); M. Luo, J.-W. Qiu, and G. Sterman, Phys. Rev. D **50**, 1951 (1994).
[11] X.-F. Guo, Phys. Rev. D **58**, 036001 (1998).
[12] R.J. Fries, B. Müller, A. Schäfer, and E. Stein, Phys. Rev. Lett. **83**, 4261 (1999).
[13] X.-F. Guo, J.-W. Qiu, and X.-F. Zhang, Phys. Rev. Lett. **84**, 5049 (2000).
[14] J.C. Collins, D.E. Soper, and G. Sterman, in *Perturbative Quantum Chromodynamics*, edited by A.H. Mueller (World Scientific, Singapore, 1989).
[15] J.-W. Qiu and G. Sterman, Nucl. Phys. **B353**, 137 (1991).
[16] M. Luo, J.-W. Qiu, and G. Sterman, Phys. Rev. D **49**, 4493 (1994).
[17] T. Matsui and H. Satz, Phys. Lett. B **178**, 416 (1986).
[18] NA38 Collaboration, M.C. Abreu *et al.*, Phys. Lett. B **444**, 516 (1998); NA38 Collaboration, M.C. Abreu *et al.*, *ibid.* **449**, 128 (1999); NA51 Collaboration, M.C. Abreu, *ibid.* **438**, 35 (1998).
[19] NA50 Collaboration, M.C. Abreu *et al.*, Phys. Lett. B **410**, 337 (1997); NA50 Collaboration, M.C. Abreu *et al.*, *ibid.* **450**, 456 (1999).
[20] X.-F. Guo, Phys. Rev. D **58**, 114033 (1998).
[21] R.K. Ellis, J. Sterling, and B. Webber, *QCD and Collider Physics* (Cambridge University Press, Cambridge, U.K., 1996).
[22] G. Atarelli, G. Parisi, and R. Petronzio, Phys. Lett. **76B**, 351 (1978); F. Khalafi and W.J. Stirling, Z. Phys. C **18**, 315 (1983); M. Beneke and V.M. Braun, Nucl. Phys. **B454**, 253 (1995).
[23] J.C. Collins, D.E. Soper, and G. Sterman, Nucl. Phys. **B308**, 833 (1988).
[24] C.T.H. Davies and W.J. Stirling, Nucl. Phys. **B244**, 337 (1984); C.T.H. Davies, W.J. Stirling, and B.R. Webber, *ibid.* **B256**, 413 (1985).
[25] G.A. Ladinsky and C.P. Yuan, Phys. Rev. D **50**, R4239 (1994).
[26] E772 Collaboration, P.L. McGaughey *et al.*, Phys. Rev. D **50**, 3038 (1994).
[27] CFS Collaboration, A.S. Ito *et al.*, Phys. Rev. D **23**, 604 (1981).
[28] E.L. Berger, L. Gordon, and M. Klasen, Phys. Rev. D **58**, 074012 (1998); **62**, 014014 (2000).
[29] P. Arnold, R.K. Ellis, and M.H. Reno, Phys. Rev. D **40**, 912 (1989); Nucl. Phys. **B330**, 284 (1990); R.J. Gonsalves, J. Pawlowski, and C.F. Wai, Phys. Rev. D **40**, 2245 (1989).
[30] X.-F. Guo, X.-F. Zhang, and W. Zhu, Phys. Lett. B **476**, 316 (2000).
[31] A.H. Mueller and J.-W. Qiu, Nucl. Phys. **B268**, 427 (1986).
[32] R. Baier, Yu.L. Dokshitzer, A.H. Mueller, S. Peigné, and D. Schiff, Nucl. Phys. **B484**, 265 (1997).
[33] A.H. Mueller, Nucl. Phys. **B558**, 285 (1999).
[34] J.M. Moss and P. L. McGaughey (private communication).
[35] E771 Collaboration, T. Alexopoulos *et al.*, Phys. Rev. D **55**, 3927 (1999).
[36] D. Kharzeev, Nucl. Phys. **A638**, 279c (1998), and references therein; S. Raha and B. Sinha, Nucl. Phys. **B198**, 543 (1987); **B218**, 413 (1989).
[37] S.J. Brodsky and A.H. Mueller, Phys. Lett. B **206**, 685 (1988).
[38] J.-W. Qiu, J.P. Vary, and X.-F. Zhang, in the proceedings of

the APS Centennial Meeting, Atlanta, GA, March 1999 (AIP Press, New York, in press); hep-ph/9809442.
[39] C. Benesh, J.-W. Qiu, and J.P. Vary, Phys. Rev. C **50**, 1015 (1994).
[40] P. L. McGaughey, J.M. Moss, and J.C. Peng, Annu. Rev. Nucl. Part. Sci. **49**, 217 (1999), and reference therein.
[41] NA10 Collaboration, P. Bordalo *et al.*, Phys. Lett. B **193**, 373 (1987).
[42] E772 Collaboration, D.M. Alde *et al.*, Phys. Rev. Lett. **66**, 133 (1991); E789 Collaboration, M.S. Kowitt *et al.*, *ibid.* **72**, 1318 (1994); Phys. Rev. D **52**, 1307 (1995).